



HAL
open science

Toward parameterization of material microstructure based on a bi-level reduced model

Liang Xia, Balaji Raghavan, Piotr Breitkopf

► **To cite this version:**

Liang Xia, Balaji Raghavan, Piotr Breitkopf. Toward parameterization of material microstructure based on a bi-level reduced model. 11e colloque national en calcul des structures, CSMA, May 2013, Giens, France. hal-01717843

HAL Id: hal-01717843

<https://hal.science/hal-01717843>

Submitted on 26 Feb 2018

HAL is a multi-disciplinary open access archive for the deposit and dissemination of scientific research documents, whether they are published or not. The documents may come from teaching and research institutions in France or abroad, or from public or private research centers.

L'archive ouverte pluridisciplinaire **HAL**, est destinée au dépôt et à la diffusion de documents scientifiques de niveau recherche, publiés ou non, émanant des établissements d'enseignement et de recherche français ou étrangers, des laboratoires publics ou privés.

Public Domain

Toward parameterization of material microstructure based on a bi-level reduced model

Liang Xia^{1,2}, Balaji Raghavan¹, Piotr Breitkopf¹

¹ Laboratoire Roberval, UMR 7337 UTC-CNRS, Université de Technologie de Compiègne, Compiègne, France

² Engineering Simulation and Aerospace Computing (ESAC), Northwestern Polytechnical University, Xi'an, China
{liang.xia, balaji.raghavan, piotr.breitkopf}@utc.fr

Résumé — The general idea here is to produce a high quality representation of the material phase indicator function of material microstructure for high resolution Digital Material Representation (DMR). The storage requirement is properly scaled down through bi-level reduction, by which the microstructure is represented in a reduced order in terms of the extracted spatial and parametric common bases. Based on the reduced data set, a parameterization model is proposed and the analysis of the intrinsic dimensionality yields the minimal set of parameters needed for the description of the microstructure with adequate precision. Moving Least Squares (MLS) is used for interpolation in this reduced space. We showcase the approach by constructing a low-dimensional model of a two-phase composite microstructure.

Mots clés — Microstructure representation, Parameterization, Model reduction, Manifold learning, Data-driven models, Moving Least Squares, Separation of variables

1 Introduction

The constant increase of computing power coupled with ever-easier access to high-performance computing platforms enables the computational investigation of materials at the microscopic level : microstructure generation and modeling [1], material property prediction and evaluation [3, 4], multi-scale analysis [5], and within a stochastic framework to include the effects of the input uncertainties at the material level in order to understand how they propagate and affect the performance of the structure [6]. At the same time, the progress in material science allows us to control the material microstructure composition to an unprecedented extent [7].

That being said, how to efficiently parameterize the microstructures under consideration is a question of significant importance. Moreover, image-based microstructure analysis, especially when it involves a large number of micrographs, requires increasingly higher memory storage requirement with the ever-increasing resolution of the micrographs provided by image techniques, such as computer tomography (CT), magnetic resonance imaging (MRI), etc.[8]. Therefore, there is also a great need to properly scale down the storage requirements for high resolution images while still maintaining a high quality representation.

In earlier works, Principal Component Analysis (PCA), has been widely used for the purpose of model reduction in structural shape design [9]. In [10], PCA has also been applied to reduce the parametric space constructed by a large-dimensional data set called the set of ‘snapshots’, e.g., M snapshots of resolution $N \times N$ (N^3 in 3D). Each snapshot may be represented as a combination of their eigen-images. For the purpose of reduction, fewer basis vectors, say m ($m \ll M$) selected in the order of decreasing importance may be used for the representation of the high-dimensional data set. With this single-level reduction, the storage requirement is then $m \times N^2 + m \times M$. In this case, the storage requirement may be a serious problem when the resolution of the image increases. This is even more critical when extending the approach to 3D with the storage requirement becoming $m \times N^3 + m \times M$, which is definitely not scalable as for $N = 1024$ and $M = 100$ some 800GB (considering 8 byte floating point numbers) are necessary for the modes alone and for $N = 4096$ and $M = 1000$, having a $\sim 50TB$ memory we go well beyond the capacity of existing workstations.

Therefore, there is a clear need for a model reduction approach that scales better with increasing re-

solution for data reduction. Using this approach, any of the microstructures under consideration could be transformed into the set of coefficients in the reduced dimension of \mathfrak{R}^m , where the coefficients may then be used for the parameterization. However, according to the discussion in [10], such a transformation is injective but *not* surjective, i.e., while every microstructure considered does correspond to a unique mapping of coefficients, an arbitrarily chosen combination of coefficients does not necessarily result in an admissible microstructure layout. In order to use the coefficients for the parameterization, certain constraints (linear, nonlinear, statistical, ...) must be enforced on the coefficients in order to construct a bijective transformation from the coefficients to the material phases layout [10, 11]. Theoretically speaking, this parameterization approach is a generalized model, which is applicable for the parameterization of microstructures of any type. However, it is too general and even redundant when considering cases where there are *intrinsic interrelationships* in the considered data set. For instance, by the thermomechanical processing of aluminum sheets, the grain structures in the rolling direction depend on the processing parameters, e.g., heating temperature, operation speed, numbers of hot and cold rollings, etc., the number of which may determine the intrinsic dimensionality of the microstructure layout [12]. Therefore, it is necessary to develop a more specific approach that can first detect the intrinsic dimensionality, and then use this to construct the parameterization model.

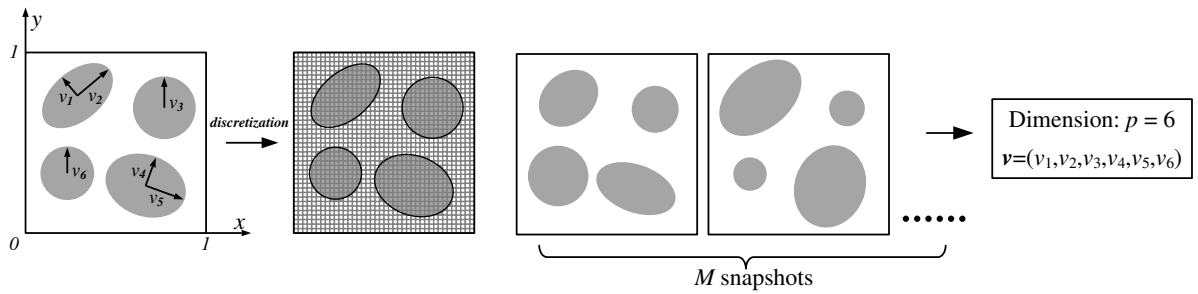


Fig. 1 – Illustration of a six-parameter microstructure and the detection of dimensionality.

For the above reasons, we have developed a bi-level reduction model, based on which a more specific parameterization model is proposed for the interrelated data set. Without loss of generality, let us consider a 2D material phase indicator function $s(x, y, \mathbf{v})$ parameterized by a certain number of parametric variables $\mathbf{v} \in \mathfrak{R}^p$, e.g., geometrical, physical, stochastic, process factors, etc. By discretization, the continuous representation turns into a snapshot $\mathbf{S}(\mathbf{v})$ of resolution $N \times N$, as shown in Fig. 1.

Using linear algebra, this discrete representation can always be transformed into the space comprised by two spatial common bases $\Phi \in \mathfrak{R}^{m_x}$ and $\Psi \in \mathfrak{R}^{m_y}$. The first level reduction is performed by choosing lower order common bases, by which the dimensionality of the data set is reduced to the order of the spatial common bases. In the second level, the reduced data set is further reduced to the order of the extracted common parametric basis $\Xi \in \mathfrak{R}^{m_e}$ and we thus have the bi-level reduced representation $\tilde{\mathbf{S}}(\mathbf{v}) = \Phi(\Xi\alpha(\mathbf{v}))\Psi^T$ in terms of bases Φ , Ψ , and Ξ . The storage requirement for this model is $(m_x + m_y) \times N + m_e \times (m_x \times m_y) + m_e \times M$, which is *significantly less* than $m \times N^2 + m \times M$ as required previously.

The developed parameterization model, which may be described as a coefficient-manifold learning approach, is constructed using the method of moving least squares (MLS) [13] or *diffuse approximation* [14]. The general idea here is to detect the intrinsic dimensionality of the data set (see Fig. 1), and then parametrize the data set in the space of the detected dimensionality. As can be seen in the aforementioned bi-level reduction process, the parametric information is contained only in the coefficients $\alpha(\mathbf{v})$ of Ξ . We first extend the algorithm of [15] to detect the intrinsic dimensionality of the coefficient-manifold. Then the MLS-based approximation is performed *locally* for the evaluation point in accordance with the detected dimensionality. By using this model, not only can arbitrary admissible microstructure micrographs be reconstructed using a limited number of parameters, but the model is also further reduced to a much lower order in accordance with the detected (intrinsic) dimensionality.

The remainder of this paper is organized in the following manner : section 2 presents general ideas and formulations. The parameterization methodology is presented in section 3. The numerical implementations for the extraction of spatial and parametric common bases is given in section 4. We demonstrate this approach by constructing a low-dimensional model of a two-phase composite microstructure in section 5. The paper ends with concluding comments and suggestions for future work.

2 Overall concept and formulation

Without loss of generality, consider a real-valued continuous or discrete material phase indicator function $s = s(x, y, \mathbf{v})$ depending on a set of intrinsic parameters $\mathbf{v} \in \mathfrak{R}^p$, e.g., geometrical, physical, stochastic, process factors, etc. Given an $N \times N$ grid of sampling points by the indicator function $[\mathbf{S}(\mathbf{v})]_{i,j} = s(x(i), y(j), \mathbf{v}), i = 1, \dots, N, j = 1, \dots, N$, continuous representation could be discretized to a representation matrix $\mathbf{S}(\mathbf{v})$, the precision of which depends on the resolution.

In practice, the discretized representations obtained using image techniques must be used instead of the continuous indicator function. Therefore, an inverse procedure must be performed by interpolation in order to obtain a continuous material phase indicator function. This spatial interpolation may be performed by using standard 2D finite element shape functions $\varphi(x, y)$

$$\tilde{s}(x, y, \mathbf{v}) = \varphi^T(x, y) \mathbf{S} \quad (1)$$

or by separating the individual spatial dimensions x and y independently

$$\tilde{s}(x, y, \mathbf{v}) = \varphi^T(x) \mathbf{S} \varphi(y) \quad (2)$$

by means of the standard 1D finite element shape functions $\varphi(x)$ and $\phi(y)$.

Using linear algebra, we can transform the $N \times N$ discrete representation $\mathbf{S}(\mathbf{v})$ in terms of two spatial common bases

$$\tilde{\mathbf{S}}(\mathbf{v}) = \Phi \mathbf{E}(\mathbf{v}) \Psi^T \quad (3)$$

where $\Phi \in \mathfrak{R}^{m_x}$ and $\Psi \in \mathfrak{R}^{m_y}$. Notice that when $m_x = m_y = N$, $\tilde{\mathbf{S}} = \mathbf{E} = \mathbf{S}$ and Φ and Ψ are identity matrices \mathbf{I} . The first level reduction is realized by choosing lower order common bases, by which the dimensionality of the data set is reduced to $m_x \times m_y$, the value of m_x and m_y depending on the degree of similarity and difference among the considered data set.

In the second level, the common parametric basis $\Xi \in \mathfrak{R}^{m_e}$ is extracted from the reduced data set

$$\tilde{\mathbf{E}}(\mathbf{v}) = \Xi \alpha(\mathbf{v}) = \alpha_1 \xi_1 + \alpha_2 \xi_2 + \dots + \alpha_{m_e} \xi_{m_e} \quad (4)$$

giving us the bi-level reduced representation

$$\tilde{\tilde{\mathbf{S}}}(\mathbf{v}) = \Phi \tilde{\mathbf{E}}(\mathbf{v}) \Psi^T = \Phi (\Xi \alpha(\mathbf{v})) \Psi^T \quad (5)$$

in terms of two spatial common bases Φ and Ψ and one parametric common basis Ξ .

As can be seen in the above bi-level reduction process, the parametric information is contained only in the coefficients $\alpha(\mathbf{v})$ of Ξ . We are thus able to build a mapping whereby each microstructure $\mathbf{v} \in \mathfrak{R}^p$ has a unique image $\alpha \in \mathfrak{R}^{m_e}$. However, there are two problems that need to be solved :

- an arbitrary $\alpha \in \mathfrak{R}^{m_e}$ does not necessarily yield an $\mathbf{v} \in \mathfrak{R}^p$,
- the dimension of \mathfrak{R}^p is not *a priori* known.

We address both problems by building a *manifold of admissible microstructures*. This is done locally for a snapshot by analyzing the local dimensionality of the space spanned by its coefficient vectors α . The detailed parameterization methodology is explained in the next section.

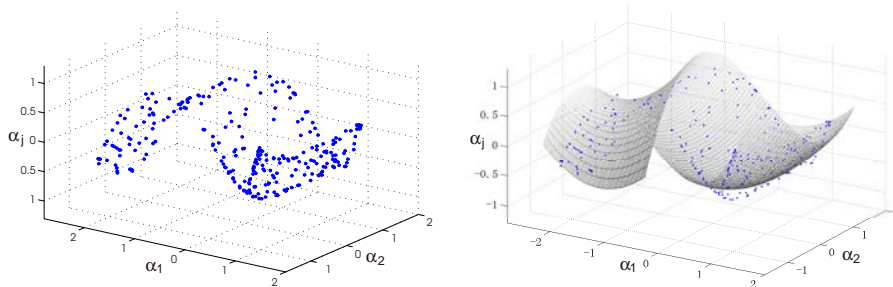


Fig. 2 – Illustration of a two dimensional α -manifold and its LS approximation.

3 The parameterization methodology

In this section, we illustrate the parameterization methodology. Based on the formulation given by Eq. (5), we only need to focus on $\alpha(\mathbf{v})$. Traditional PCA based model reduction would stop at Eq.(5) and use the coefficients $\alpha = [\alpha_1, \alpha_2, \dots, \alpha_{m_e}]$ as the design variables for parameterization. However, the coefficients can not be directly interpreted as design variables without taking into account the possible inter-relationships that exist between them so as to render feasible shapes. This means that we now need to take a closer look at the α 's obtained from the M snapshots in order to detect the true dimensionality (p) of the design domain. For the sake of simplicity and ease of visualization, we assume that the order of the parametric space is $\mathbf{v} \in \mathbb{R}^2$. Considering a large-dimensional admissible data set generated by the so called ‘snapshots’ method, the corresponding α -manifold is shown in Fig. 2 together with its global approximation using the method of Least Squares (LS) with a third order polynomial.

From Fig. 2, it can be seen that the α 's form a set of two-dimensional manifolds rather than a cloud of points in 3D space, clearly indicating that the dimensionality of the parametric space is two, as is known *a priori*. The coefficients may then be expressed as a function of two chosen coefficients, e.g., $\alpha_j = \alpha_j(\alpha_1, \alpha_2)$, $j = 3, \dots, m_e$ by this global approximation. However, it is not practical to globally approximate the manifold when it comes to cases of higher dimensionality and more complexity. Therefore, instead of pursuing a global approximation, a more practical solution would be a local approximation using the method of Moving Least Squares (MLS). The MLS-based approximation is performed locally for the evaluation point in accordance with the detected dimensionality. The general concept is illustrated in Fig. 3, where only a limited number of red points are needed for local approximation instead of the whole data set of blue points.

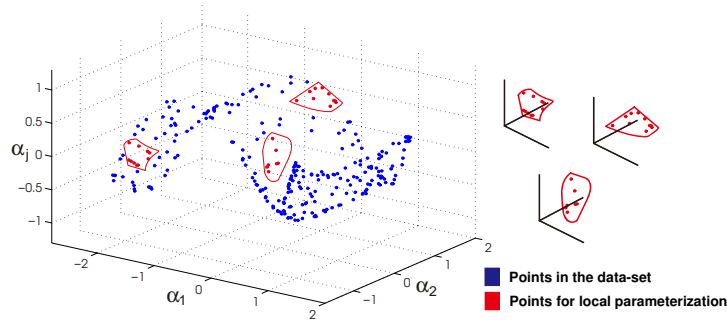


Fig. 3 – Illustration of the concept of local approximation.

In order to detect the intrinsic dimensionality of the α -manifolds, we extend the work of [15]. To locally detect the dimensionality of the hyper-surface in the neighborhood of the evaluation point α^{ev} , a sufficiently dense local neighborhood is generated by sampling the nbd neighboring points $\beta_1, \beta_2, \dots, \beta_{nbd}$ in the parametric space. We next use a polynomial basis centered on α^{ev}

$$\mathbf{P} = \begin{bmatrix} 1 & \beta_1^1 - \alpha_1^{ev} & \beta_2^1 - \alpha_2^{ev} & \dots & \beta_{m_e}^1 - \alpha_{m_e}^{ev} \\ \vdots & \vdots & \vdots & \dots & \vdots \\ 1 & \beta_1^{nbd} - \alpha_1^{ev} & \beta_2^{nbd} - \alpha_2^{ev} & \dots & \beta_{m_e}^{nbd} - \alpha_{m_e}^{ev} \end{bmatrix} \quad (6)$$

with an appropriate weighting function (e.g. Gaussian $w(d) = \exp(-c \times d^2)$ where d is the distance from node and c determines the ‘‘strength’’ of influence of the node) and assemble the moment matrix $\mathbf{A} = \mathbf{P}^T \mathbf{W} \mathbf{P}$, where \mathbf{W} is the diagonal matrix whose elements correspond to the weighted contributions of the neighboring nodes. Finally, we detect the local rank of the manifold by calculating the singular values of the moment matrix \mathbf{A} , this gives us the dimensionality $p \leq m_e$.

4 The extraction of common bases

4.1 Level 1 : Spatial common bases extraction

A given real-valued matrix may be decomposed using Singular Value Decomposition (SVD) in terms of its ‘left’ and ‘right’ singular vectors, and the ‘central’ diagonal matrix, i.e. $\mathbf{S} = \mathbf{U} \mathbf{\Sigma} \mathbf{V}^T$. In the first level

reduction, the spatial common bases Φ and Ψ are extracted from the two groups of ‘left’ and ‘right’ singular vectors \mathbf{U}_k and \mathbf{V}_k , $k = 1, \dots, M$ and M is the number of considered snapshots.

Consider a set of discrete $2D$ $N \times N$ snapshots \mathbf{S}_k ($k = 1, \dots, M$) and their average $\bar{\mathbf{S}} = \sum_{k=1}^M \mathbf{S}_k / M$. By retaining the first m_k left and right singular vectors corresponding to the m_k largest singular values in SVD, each centered snapshot may be expressed as

$$\mathbf{S}_k - \bar{\mathbf{S}} = \mathbf{U}_k \Sigma_k \mathbf{V}_k^T, \quad k = 1, 2, \dots, M \quad (7)$$

where the value of $m_k \leq N$ depends on the material layout of the snapshot.

The model reduction in this stage is to represent all the ‘‘left’’ and ‘‘right’’ singular vectors by a linear combination of lower dimensional Φ and Ψ , separately. Principle Component Analysis (PCA) is applied for the extraction of Φ and Ψ . In this paper, we only provide the extraction process for Φ , since Ψ can be obtained by a similar approach. We first calculate the deviation and covariance matrices \mathbf{D}_U and \mathbf{C}_U for the ‘‘left’’ singular vectors $\mathbf{U}_1, \mathbf{U}_2, \dots, \mathbf{U}_M$:

$$\mathbf{D}_U = [\mathbf{U}_1 \mathbf{U}_2 \dots \mathbf{U}_M] \quad \text{and} \quad \mathbf{C}_U = \mathbf{D}_U \mathbf{D}_U^T \quad (8)$$

allowing us to express any \mathbf{U}_k in terms of the eigenvectors ϕ_i of \mathbf{C}_U

$$\mathbf{U}_k = \sum_{i=1}^N \mathbf{A}_{ik} \phi_i, \quad \mathbf{A}_{ik} = \phi_i^T \mathbf{U}_k \quad (9)$$

Notice that the assembly of ‘‘left’’ singular vectors directly gives the deviation matrix since the deviation has already been taken in Eq.(7). Retaining the first m_x most ‘‘energetic’’ modes, we have the the common vector basis Φ expressed

$$\Phi = [\phi_1, \phi_2, \dots, \phi_{m_x}] \quad (10)$$

By similar extraction process, we have another common vector basis $\Psi = [\psi_1, \psi_2, \dots, \psi_{m_y}]$ and its coefficients \mathbf{B}_k , $k = 1, 2, \dots, M$. The matrices \mathbf{U}_k and \mathbf{V}_k may now be approximated in terms of the two separate bases Φ and Ψ

$$\mathbf{U}_k \approx \Phi \mathbf{A}_k, \quad \mathbf{A}_k = \Phi^T \mathbf{U}_k \quad (11)$$

$$\mathbf{V}_k \approx \Psi \mathbf{B}_k, \quad \mathbf{B}_k = \Psi^T \mathbf{V}_k \quad (12)$$

Substituting the above into Eq.(7), we get

$$\tilde{\mathbf{S}}_k = \bar{\mathbf{S}} + \Phi \mathbf{E}_k \Psi^T \quad (13)$$

where

$$\mathbf{E}_k = \mathbf{A}_k \Sigma_k \mathbf{B}_k^T, \quad k = 1, 2, \dots, M \quad (14)$$

The dimensionality of matrix \mathbf{E}_k is $m_x \times m_y$.

4.2 Level 2 : Parametric common basis extraction

In the second level, further reduction is achieved by using a standard POD reduction approach [9] on the reduced data set obtained by former level. Each $m_x \times m_y$ reduced matrix \mathbf{E}_k is restored in a column vector \mathbf{e}_k of length $m_x \times m_y$. Similar to the calculation of the deviation and covariance matrices, we have matrices \mathbf{D}_e and \mathbf{C}_e

$$\mathbf{D}_e = [\mathbf{e}_1, \mathbf{e}_2, \dots, \mathbf{e}_M] \quad \text{and} \quad \mathbf{C}_e = \mathbf{D}_e \mathbf{D}_e^T \quad (15)$$

Without loss of generality, we assume $m_x \leq m_y$, we can express \mathbf{e}_k in terms of its eigenvectors extracted by PCA.

$$\mathbf{e}_k = \sum_{i=1}^{m_x} \alpha_{ik} \xi_i, \quad \alpha_{ik} = \xi_i^T \mathbf{e}_k \quad (16)$$

Taking a reasonable assumption that $M \ll (m_x \times m_y)$, we define a projection basis $\Xi = [\xi_1, \xi_2, \dots, \xi_{m_e}]$, where $m_e \ll M$. An arbitrary \mathbf{e}_k is approximated by

$$\tilde{\mathbf{e}}_k = \sum_{i=1}^{m_e} \alpha_{ik} \xi_i = \Xi \alpha_k \quad (17)$$

By transforming the approximated vector $\tilde{\mathbf{e}}_k$ back to the matrix form $\tilde{\mathbf{E}}_k$, an arbitrary centered snapshot is approximated by

$$\tilde{\mathbf{S}}_k = \bar{\mathbf{S}} + \Phi \tilde{\mathbf{E}}_k \Psi \quad (18)$$

The general averaged image reconstruction error is measured by

$$\varepsilon = \frac{\sum_{k=1}^M (\mathbf{S}_k - \tilde{\mathbf{S}}_k)^T (\mathbf{S}_k - \tilde{\mathbf{S}}_k)}{\sum_{k=1}^M (\mathbf{S}_k - \bar{\mathbf{S}})^T (\mathbf{S}_k - \bar{\mathbf{S}})} \quad (19)$$

where \mathbf{S}_k and $\tilde{\mathbf{S}}_k$ are the original and reconstructed snapshot, respectively. The accuracy of the reconstruction depends on two parts : m_x and m_y in the first level and m_e in the second level. By the proposed two-level reduction model, the storage requirement is reduced to $(m_x + m_y) \times N + m_e \times (m_x \times m_y) + m_e \times M$ in 2D case. Moreover, further reductions may be achieved for anisotropic materials when $m_x \neq m_y$.

5 Numerical test case

We consider a commonly analyzed periodic two-phase microstructure pattern as shown in Fig. 4. Microstructures of such pattern can be used to model various types of materials, such as fiber composites [4], and reinforced alloys [16]. By relating the circular radii to two random variables, 500 snapshots of resolution 256×256 have been generated in grayscale [0 255]. By excluding the snapshots where there are overlaps among the circular inclusions as *inadmissible*, we are left with 278 admissible snapshots.

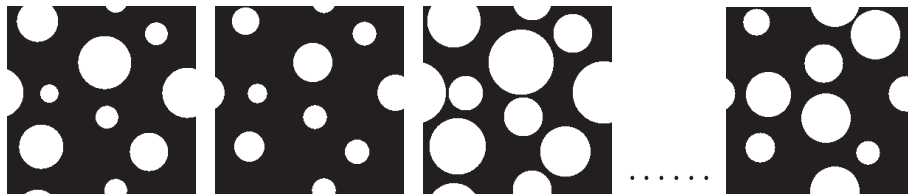


Fig. 4 – Admissible microstructure snapshots.

In the first level reduction, SVD is performed for each snapshot. Since we have no intention of reducing the model in this stage, the first m_k most “energetic” left and right singular vectors are retained for each snapshot and thereafter no reconstruction error is introduced here. The value of $m_k \leq N$ depends on the layout of the material phases. The averaged value of retained modes here is 143, where the lowest and largest value are 96 and 167 respectively. The spatial common bases Φ and Ψ are extracted from the retained left and right singular vectors, respectively. For the purpose of a better visualization, assume $m_x = m_y$ in snapshot reconstruction and the corresponding error curve is given in Fig. 5(a). It can be seen that the retained left and right singular vectors can be represented by the two basis of reduced dimensionality ($m_x = m_y \leq N$) within an acceptable degree of reconstruction error. Note that, m_x doesn’t have to equal m_y , especially when anisotropic materials are considered and obviously, the microstructure considered here is anisotropic. Fig. 5(b) and (c) shows the reconstruction error versus m_x and m_y chosen independently. This means that a further reduction in storage requirement may be achieved by choosing m_x and m_y independently. The reconstructed snapshots are shown in Fig. 5 from (d) to (g).

In the second level reduction, POD reduction is performed on the reduced data set. Without loss of generality, the dimensionality of the two bases Φ and Ψ in the former level is chosen to be $m_x = m_y = 150$, which introduces an initial error of 5.1% as shown by comparing Fig. 6(b) and (c). However, an error of this degree doesn’t affect us too much as long as the reconstructed figure describes the general layout of material phases, since the image can always be refined by post-progressing operations, such as filtering, boundary and corner enhancement [17]. The reconstruction error versus m_e is given by Fig. 6(a), where the error decreases sharply over the first 20 modes. The corresponding reconstructed snapshots are given from Fig. 6(d) to (h), where the number of retained modes varies from 1 to 100. Based on the POD reduction process, the dimensionality of the data set could be reduced to 20 without any further loss of image information except for the initial 5.1%.

From Fig. 7, we can see that the α ’s form a set of two-dimensional manifolds rather than a cloud of points in 3D space *regardless of the particular triplet of modes used*, clearly indicating that the dimensionality of the design domain is **two**. We do know this beforehand, since the generated snapshots given in

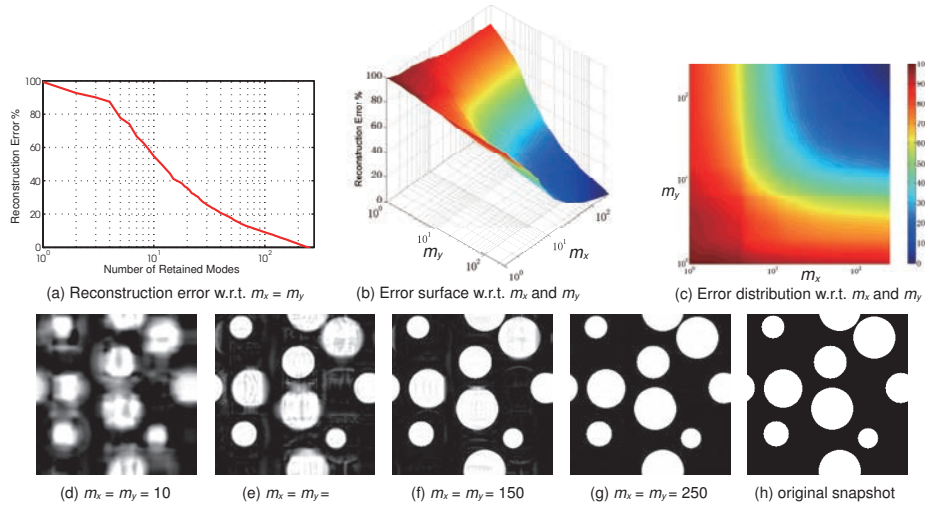


Fig. 5 – Reconstruction error w.r.t. m_x and m_y and reconstructed snapshots.

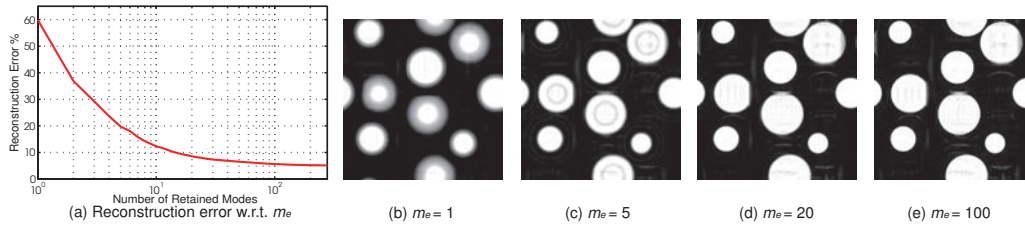


Fig. 6 – Reconstruction error w.r.t. m_e and reconstructed snapshots.

Fig. 4 is in fact uniquely parametrized by linking the two random variables to the radii of circular inclusions. In other words, we have $\alpha_j = \alpha_j(\alpha_1, \alpha_2)$, $j = 3, \dots, m_e$ through MLS-based local approximation and accordingly an arbitrary microstructure snapshot can be expressed as $\mathbf{S} = \mathbf{S}(\alpha_1, \alpha_2)$ with a pair of particular value for α_1 and α_2 . In this case, we retain the first $m_e = 30$ modes according to the reconstruction error curve in Fig. 6. As can be seen in Fig. 7, the data set composed by admissible snapshots is implicitly constrained in a non-convex hull, i.e. points in the hull correspond to admissible microstructures, while points outside correspond to inadmissible microstructures. For arbitrarily chosen admissible values of α_1 and α_2 , e.g. points **a**, **b**, and **c** in Fig. 7, corresponding microstructures are obtained through the parameterization model.

6 Conclusion and perspectives

This work has proposed an original parameterization model for material microstructures based on a bi-level reduced order model. The original data set composed of snapshots is first reduced in two levels through the extraction of both spatial and parametric common bases. Next, by detecting the intrinsic dimensionality of the data set, MLS is applied for the approximation of the coefficient-manifolds. Using this model, an arbitrary admissible microstructure can be reconstructed with a limited number of parameters with adequate accuracy of representation. This parameterization model may be used as input for the evaluation and optimization of material effective properties. Moreover, further work needs to be performed for the bi-level reduction model in accordance with 3D tensor decomposition for three-dimensional microstructures.

Acknowledgements

This research was conducted as part of the OASIS project, supported by OSEO within the contract FUI no. F1012003Z, and carried out in the framework of the Labex MS2T, which was funded by the French Government, through the program “Investments for the future” managed by the National Agency for Research (Reference ANR-11-IDEX-0004-02). The first author is grateful to the China Scholarship Council (CSC) for its financial assistance.

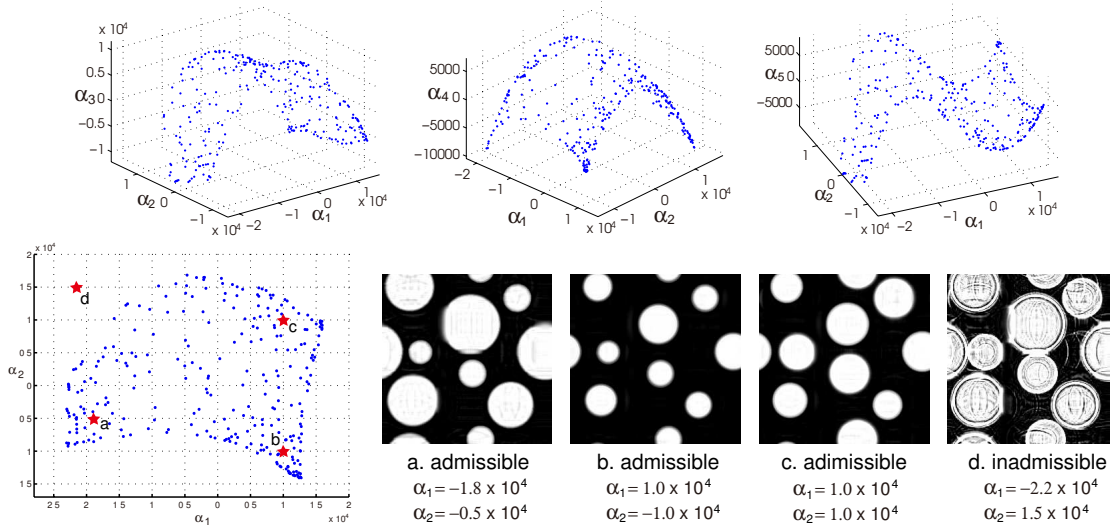


Fig. 7 – 2D α -manifolds of snapshots in Fig. 4 and parameterization

Références

- [1] Y. Xu and W. Zhang. Numerical modelling of oxidized microstructure and degraded properties of 2d c/sic composites in air oxidizing environments below 800 °C. *Mater. Sci. Eng., A*, 528(27) :7974–7982, 2011.
- [2] S. Guessasma, P. Babin, G. Della Valle, and R. Dendieue. Relating cellular structure of open solid food foams to their young’s modulus : Finite element calculation. *Int. J. Solids Struct.* , 45(10) :2881–2896, 2008.
- [3] Y. Xu and W. Zhang. A strain energy model for the prediction of the effective coefficient of thermal expansion of composite materials. *Comp. Mater. Sci.*, 53(1) :241–250, 2012.
- [4] J. Zeman and M. Sejnoha. Numerical evaluation of effective elastic properties of graphite fiber tow impregnated by polymer matrix. *J. Mech. Phys. Solids*, 49(1) :69–90, 2001.
- [5] F. Feyel and J. Chaboche. FE² multiscale approach for modelling the elastoviscoplastic behaviour of long fibre sic/ti composite materials. *Comput. Methods Appl. Mech. Eng.*, 183(3-4) :309–330, 2000.
- [6] B. Velamuri Asokan and N. Zabaras. A stochastic variational multiscale method for diffusion in heterogeneous random media. *J. Comput. Phys.*, 218(2) :654–676, 2006.
- [7] D. T. Fullwood, S. R. Niezgod, B. L. Adams, and S. R. Kalidindi. Microstructure sensitive design for performance optimization. *Prog. Mater. Sci.*, 55(6) :477–562, 2010.
- [8] S. Ghosh and D. Dimiduk. *Computational Methods for Microstructure-Property Relationships*. Springer, New York, 2011.
- [9] B. Raghavan, M. Hamdaoui, M. Xiao, P. Breitenkopf, and P. Villon. A bi-level meta-modeling approach for structural optimization using modified pod bases and diffuse approximation. *Comput. Struct.*, 2013. Article in Press.
- [10] B. Ganapathysubramanian and N. Zabaras. Modeling diffusion in random heterogeneous media : Data-driven models, stochastic collocation and the variational multiscale method. *J. Comput. Phys.*, 226(1) :326–353, 2007.
- [11] B. Ganapathysubramanian and N. Zabaras. A non-linear dimension reduction methodology for generating data-driven stochastic input models. *J. Comput. Phys.*, 227(13) :6612–6637, 2008.
- [12] O. Engler and J. Hirsch. Texture control by thermomechanical processing of aa6xxx al-mg-si sheet alloys for automotive applications – a review. *Mater. Sci. Eng., A*, 336(1-2) :249–262, 2002.
- [13] P. Lancaster and K. Salkauskas. Surfaces generated by moving least squares methods. *Math. Comput.*, 87 :141–158, 1981.
- [14] B. Nayroles, G. Touzot, and P. Villon. Generalizing the finite element method : Diffuse approximation and diffuse elements. *Comput. Mech.*, 10(5) :307–318, 1992.
- [15] K. Fukunaga and D.R. Olsen. An algorithm for finding intrinsic dimensionality of data. *IEEE T. Comput.*, C-20(2) :176–183, 1971.
- [16] S. Ghosh, K. Lee, and P. Raghavan. A multi-level computational model for multi-scale damage analysis in composite and porous materials. *Int. J. Solids Struct.* , 38(14) :2335–2385, 2001.
- [17] T. Law and H. Itoh and H. Seki. Image filetering, edge detection, and edge tracing using fuzzy reasoning. *IEEE Trans. Pattern. Anal. Mach. Intell.*, 18(5) :481–491, 1996.